

Light propagation in twisted anisotropic media: Application to photoreceptors

Peter McIntyre

Max-Planck-Institut für biologische Kybernetik, Spemannstrasse 38, 7400 Tübingen, West Germany

Allan W. Snyder

Institute of Advanced Studies, Departments of Applied Mathematics and Neurobiology, Australian National University, P.O. Box 4, Canberra, A.C.T. 2600 Australia

(Received 28 June 1977)

The propagation of light through a slowly twisting anisotropic medium is described by a coupled-mode theory; expressions are derived for the electric field for the case of a birefringent dichroic medium with a constant rate of twist. The method provides a simple and intuitive means for determining the effect of twisting on the linear birefringence and dichroic absorption of the medium, particularly when the light is initially linearly polarized. The theory is well suited to the analysis of light absorption in twisting insect photoreceptors, such as found in bees and ants. We provide full expressions and useful approximations for the polarization sensitivity and the initial direction of polarization to give maximum absorption for several types of photoreceptors.

Several interesting properties are exhibited by an anisotropic medium that twists about the direction of the advancing wave. In general an incident linearly polarized wave becomes elliptically polarized, and the polarization ellipse rotates as the wave propagates through the medium. This latter property, normally associated with optically active material, is in this case due to the microscopic structure of the medium rather than to the properties of the molecules—hence the name form optical rotation.¹ The theory is well known, especially in the context of liquid crystals, in which the rate of twist may be large.²⁻⁵

Our interest in twisted media arises from a determination of the absorption of polarized light in twisting insect photoreceptors, in which the rate of twist is small.⁶⁻⁸ For this case, a coupled-mode theory displays most easily the effect of twisting on such properties of the medium as dichroic absorption and birefringence. We find also elliptical polarization in general and form optical rotation, and in a certain limit that a linearly polarized incident wave remains linearly polarized and rotates at the same rate as the medium twists. This limit first discussed by Mauguin⁹ in 1911 seems to have received little attention since. Other possible applications of this slow-twist method may be to optical waveguides with a crystalline core¹⁰ and to liquid crystals in general.

The full coupled-mode equations are a reformulation of Maxwell's equations and can in principle be solved to give exact solutions. However, for the condition of a slow twist this full solution contains more information than is normally required and is therefore unnecessarily complicated. We make use of the weak-coupling approximation,^{6,11,12} in which reflected waves are neglected, to simplify the solution.

A linearly polarized wave propagating parallel to an optical axis of a nontwisted, linearly birefringent and dichroic medium remains linearly polarized as it travels through the medium. However if the medium is twisted, there is in general no optical axis; an incident wave becomes elliptically polarized as it propagates through the medium. The normal modes of a twisted medium are elliptically polarized in contrast to a nontwisted uniform

medium for which linearly polarized normal modes can be found.

Figure 1(a) shows the situation for a twisted medium. Waves propagate in the z direction and the two axes $\mathbf{x}(z)$, $\mathbf{y}(z)$ (the optical axes of the untwisted medium, now the axes of the polarization ellipses of the normal modes) rotate as the medium twists. At any position z in the medium, the field can be resolved into two plane waves, one with \mathbf{E} parallel to $\mathbf{x}(z)$ the other with \mathbf{E} parallel to $\mathbf{y}(z)$. Twisting of the medium causes these two plane waves to interchange their energy (couple) as they propagate. Use of the twisting waves allows us to include linear birefringence and dichroism in a simple way.

1. COUPLED-MODE THEORY

Consider a stack of birefringent plates each of thickness δz , and let the optical axes $\hat{\mathbf{x}}$, $\hat{\mathbf{y}}$ of each plate be at an angle $\delta\Omega$ to those of the preceding plate [Fig. 1(b)]. The electric fields propagating in the $+z$ direction in two adjacent plates A , B are given by expressions of the form

$$\mathbf{E}_A(z) = a_x \hat{\mathbf{x}}_A e^{i\bar{\beta}_x z} + a_y \hat{\mathbf{y}}_A e^{i\bar{\beta}_y z}, \quad (1)$$

$$\mathbf{E}_B(z) = (a_x + \delta a_x) \hat{\mathbf{x}}_B e^{i\bar{\beta}_x z} + (a_y + \delta a_y) \hat{\mathbf{y}}_B e^{i\bar{\beta}_y z}, \quad (2)$$

where $\bar{\beta}_x$, $\bar{\beta}_y$ are the propagation constants for light polarized in the $\hat{\mathbf{x}}$, $\hat{\mathbf{y}}$ directions, respectively, and the two sets of axes are related by

$$\hat{\mathbf{x}}_A = \hat{\mathbf{x}}_B \cos \delta\Omega - \hat{\mathbf{y}}_B \sin \delta\Omega, \quad (3)$$

$$\hat{\mathbf{y}}_A = \hat{\mathbf{x}}_B \sin \delta\Omega + \hat{\mathbf{y}}_B \cos \delta\Omega. \quad (4)$$

By matching the electric field at the boundary, putting

$$A_x(z) = a_x(z) e^{i\bar{\beta}_x z}, \quad (5)$$

$$A_y(z) = a_y(z) e^{i\bar{\beta}_y z}, \quad (6)$$

taking the limit $\delta z \rightarrow 0$ and assuming a linear twist $\Omega(z) = \xi z$, we arrive at the coupled-mode equations

$$\frac{dA_x}{dz} - i\bar{\beta}_x A_x = \xi A_y, \quad (7)$$

$$\frac{dA_y}{dz} - i\bar{\beta}_y A_y = -\xi A_x. \quad (8)$$

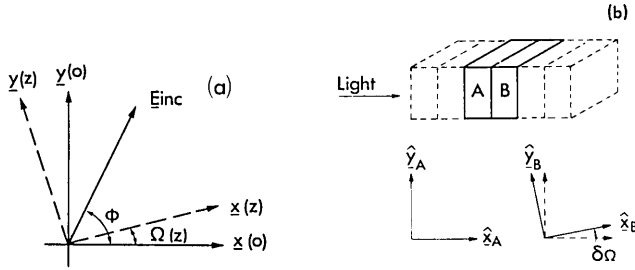


FIG. 1. (a) Coordinate system for a twisted medium; (b) stack of birefringent plates; the optical axes of each plate are rotated $\delta\Omega$ with respect to the previous plate.

In order to be able to neglect the interchange of energy between forward (+z) and backward (-z) traveling waves, we have assumed that $|\xi| < |\bar{\beta}_x|$, $|\bar{\beta}_y|$ and that

$$|(\bar{\beta}_x - \bar{\beta}_y)/(\bar{\beta}_x + \bar{\beta}_y)| \ll 1.$$

The first inequality is satisfied if we assume a slow twist rate ξ but, as $|\beta_x|, |\beta_y| \geq 12 \text{ rad}/\mu\text{m}$, this assumption is not greatly restrictive. The second assumption is satisfied provided that the birefringence is small and the absorption coefficient small compared to $|\beta_x|, |\beta_y|$. Equations (7) and (8) describe the propagation of plane waves in the +z direction through a continuously twisting medium with a twist rate of ξ rad per unit length (about the z axis) and propagation constants $\bar{\beta}_x, \bar{\beta}_y$ along the (twisting) coordinate axes $\hat{x}(z), \hat{y}(z)$. Solution of these equations, e.g., by the Laplace transform method, is straightforward, giving

$$A_x(z) = \{p \cos(\xi z/\sqrt{F}) + \sqrt{F}(ip\bar{X} + q) \sin(\xi z/\sqrt{F})\} e^{i\bar{\beta}_s z}, \quad (9)$$

$$A_y(z) = \{q \cos(\xi z/\sqrt{F}) - \sqrt{F}(p + iq\bar{X}) \sin(\xi z/\sqrt{F})\} e^{i\bar{\beta}_s z}, \quad (10)$$

where

$$\bar{\beta}_s = \frac{1}{2}(\bar{\beta}_x + \bar{\beta}_y), \quad (11)$$

$$\bar{X} = (\bar{\beta}_x - \bar{\beta}_y)/2\xi, \quad (12)$$

$$F = (1 + \bar{X}^2)^{-1}, \quad (13)$$

$$p = A_x(0), \quad (14)$$

$$q = A_y(0). \quad (15)$$

Unity initial power requires $\frac{1}{2}(|p|^2 + |q|^2) = 1$. If the initial field is linearly polarized at an angle ϕ to $\mathbf{x}(0)$, $p = \sqrt{2} \cos\phi$ and $q = \sqrt{2} \sin\phi$. We allow for absorbing media by writing

$$\bar{\beta}_j = \beta_j + \frac{1}{2}i\alpha_j, \quad j = x \text{ or } y, \quad (16)$$

where, for an infinite medium, $\beta_j = 2\pi n_j/\lambda$, n_j is the refractive index of the medium, α_j is the absorption coefficient for light linearly polarized in the j th direction, and we have assumed $\alpha_j \ll \beta_j$.¹³

The time-averaged power $P(z)$ over the infinite cross section is given by

$$P(z) = \frac{1}{2}[|A_x(z)|^2 + |A_y(z)|^2]. \quad (17)$$

Expressions for $P(z)$ and the time-averaged power absorbed are given by Eqs. (A1)–(A3) in the Appendix. If the medium is only birefringent ($\alpha_x = \alpha_y$) or only dichroic ($n_x = n_y$), the expressions for the power are greatly simplified.

The above solution assumes a linear twist, i.e., ξ is a constant. Unfortunately there is no analytical solution

for the case $\xi = \xi(z)$, except when $\bar{\beta}_x = \bar{\beta}_y$. This is a trivial case in which the twisting of the medium has no effect on the propagating waves.

The above theory can be directly extended to a twisted optical waveguide propagating only the fundamental mode, if the difference between the refractive index of the waveguide and that of the surrounding medium is small, and if the surrounding medium is either isotropic or twists with the waveguide. Then the waveguide mode is approximately uniformly linearly polarized in the transverse plane,^{14,15} and all equations except Eqs. (1), (2), and (16) are unchanged. In Eqs. (1) and (2) the unit vectors $\hat{x}_A, \hat{y}_A, \hat{x}_B, \hat{y}_B$ and $\hat{x}(z), \hat{y}(z)$ must be replaced by the appropriate modal electric vector $\mathbf{e}(x, y)$. In Eq. (16), α_j is replaced by $\eta\alpha_j$, where η is the fraction of modal power within the waveguide,^{14,16,17} and β_j is now the modal propagation constant, a function of the refractive indexes of the waveguide and the surround.¹⁴ The birefringence of the waveguide medium will therefore enter the calculations in a slightly more complicated way than for the infinite medium. In many cases $\eta \approx 1$ and the infinite-medium approximation to the waveguide is then sufficiently accurate.

II. POLARIZATION PARAMETERS

The electromagnetic field in a twisted anisotropic medium is in general elliptically polarized, and both the ellipticity σ ,¹⁸ and the angle Ψ between the major axis of the polarization ellipse and the rotating $\mathbf{x}(z)$ axis are functions of z . The expressions for σ and Ψ are well-known,^{19,20} and in our notation are

$$\tan 2\Psi = \frac{2 \operatorname{Re}(A_x A_y^*)}{|A_x|^2 - |A_y|^2}, \quad (18)$$

$$\sigma = \tan \left[\frac{1}{2} \sin^{-1} \left(\frac{2 \operatorname{Im}(A_x A_y^*)}{|A_x|^2 + |A_y|^2} \right) \right], \quad (19)$$

where Re, Im are the real and imaginary parts, respectively. If we assume a lossless medium and a field initially linearly polarized at an angle ϕ to $\mathbf{x}(0)$,

$$\tan 2\Psi = \frac{\sin 2\phi \cos 2\tau z - \sqrt{F} \cos 2\phi \sin 2\tau z}{F \cos 2\phi (\cos 2\tau z + X^2) + \sqrt{F} \sin 2\phi \sin 2\tau z}, \quad (20)$$

$$\sigma = \tan \left(\frac{1}{2} \sin^{-1} \left\{ [2X\sqrt{F} \sin \tau z (\sin 2\phi \cos \tau z - \sqrt{F} \cos 2\phi \sin \tau z)] \right\} \right), \quad (21)$$

where $\tau = \xi/\sqrt{F}$, and $\sigma > 0$ corresponds to right-hand elliptically polarized light.²⁰ Equations (20) and (21) are in agreement with the corresponding expressions found from the differential-equation formulation of Ref. 5.

III. NORMAL MODES

A useful alternative way to analyze propagation in a twisted medium is to use the normal modes.^{1,3} In a lossless medium the normal modes propagate unchanged, except in phase, in contrast to the rotating modes used above, which exchange energy as they propagate (i.e., are not true modes of the system). The normal modes may be found by diagonalizing the coupled-mode equations, Eqs. (7) and (8), and, in a lossless medium, have the form

$$\psi_{1,2}(z) = \{\hat{x}(z) - i[X \pm (1 + X^2)^{1/2}] \hat{y}(z)\} e^{i(\beta_x \pm \tau)z}, \quad (22)$$

where the upper (lower) signs refer to mode 1 (2). In a lossless medium, $X = (\beta_x - \beta_y)/2\xi$ and τ are real. These normal modes are in general elliptically polarized, and the axes of their polarization ellipses rotate at the same rate as the medium twists. The two modes have the same ellipticity but their major axes are perpendicular and the \mathbf{E} vectors rotate in opposite directions. They propagate at different velocities because of the $\pm \tau$ in the exponent.

IV. DISCUSSION

Before going on to apply the theory to twisted photoreceptors, we first discuss two interesting limits. In general an initially linearly polarized field becomes elliptically polarized and the polarization ellipse rotates as the field propagates through the twisted medium. However in the following two cases, the field remains approximately linearly polarized for all z .

(i) $\Delta\beta/2\xi = (\beta_x - \beta_y)/2\xi \gg 1$. In this limit the normal modes are approximately linearly polarized (in the limit $\Delta\beta/2\xi \rightarrow \infty$ they are identical to the rotating modes), but still have a z -dependent phase difference, giving rise to elliptical polarization in general:

$$\tan 2\Psi = \tan 2\phi \cos \Delta\beta z + O(2\xi/\Delta\beta), \quad (23)$$

$$\sigma = \tan^{-1}[\frac{1}{2} \sin^{-1}(\sin 2\phi \sin \Delta\beta z)] + O(2\xi/\Delta\beta). \quad (24)$$

However if only one of the normal modes is excited ($\phi = 0, \pi/2$), the field remains linearly polarized for all z (i.e., $\sigma = 0$), and the direction of polarization rotates at the same rate as the medium twists ($\Psi = 0$). Equations (23) and (24) are a good approximation to the exact expressions Eqs. (20) and (21) when $\Delta\beta/2\xi \geq 10$. This limit was discussed by Mauguin⁹ in 1911 but does not seem to have received much attention in the literature since.

(ii) $\Delta\beta/2\xi \ll 1$. Here the normal modes are approximately circularly polarized in opposite directions, resulting in a linearly polarized field. The direction of polarization rotates slowly as the field propagates through the twisted medium, owing to the difference in the propagation velocities of the two normal modes. This limit is discussed in some detail in Ref. 1.

V. APPLICATION TO PHOTORECEPTORS

As an interesting application of the theory, we now examine the absorption of light in twisted insect photoreceptors. These have been observed in the worker

bee^{8,21} and in the bulldog ant^{22,23}; in both cases it is found that the twist rate is small ($\sim 1^\circ/\mu\text{m}$) and approximately constant. Photoreceptors are known to be dichroic and birefringent, and the response of insects to linearly polarized light is of particular interest, so that our coupled-mode theory is especially suited to this task.

Insect photoreceptors or rhabdomeres occur either in the form of an open rhabdom as in fly (see Fig. 2) in which the individual rhabdomeres are separated, or fused together in groups to form fused rhabdoms, as in ant or bee (see Figs. 4–6). In both cases the rhabdomeric medium consists of aligned, thin, tubular membranes, the microvilli, which contain the photopigment. The alignment of the dipole axes of the chromophore groups of the photopigment molecules within the microvilli, together with the structure and arrangement of the microvilli, give rise to the dichroic absorption of the rhabdomeres,²⁴ which is characterized by the dichroic ratio $\Delta = \alpha_{\parallel}/\alpha_{\perp}$, where α_{\parallel} , α_{\perp} are the absorption coefficients of the medium when the light is polarized parallel and perpendicular, respectively, to the microvilli. Measurements on various insects indicate a value $\Delta \sim 10$ for rhabdomeres in fused rhabdoms, but the evidence is not yet conclusive.²⁵ A value $\Delta \sim 2$ is generally assumed for fly rhabdomeres.

The birefringence of the rhabdomeric medium arises from the intrinsic birefringence of the microvilli membrane, and from the structure and arrangement of the microvilli (form birefringence).²⁴ The total birefringence (intrinsic + form) measured in fly rhabdomeres²⁶ is $\Delta n \sim 4 \times 10^{-3}$.

Twisting is of particular relevance to the polarization sensitivity (PS) of insect photoreceptors (see Appendix for definition). An individual retinula cell is theoretically sensitive to the direction of polarization because of the dichroic absorption properties of its rhabdomere.²⁷ Such sensitivity is often not observed, indicating that the PS of the retinula cell is somehow destroyed. Twisting of the rhabdom is one possible way to account for this. Other possibilities are discussed in Ref. 22.

A preliminary theoretical analysis⁷ has already shown that twisting reduces the PS of retinula cells in a symmetric fused rhabdom, and more recently a detailed account of PS in twisted bee rhabdoms has appeared.⁸ In this section we give a general treatment of how the theory is applied to photoreceptors, in effect extending the simple case of Ref. 7 to include the varying degrees of anisotropy found in rhabdoms. Analytic expressions are found for all cases. A more detailed account of specific rhabdoms is in preparation. An important result of this section is that the simple expression for the PS of a symmetric fused rhabdom is often a good approximation to the more complicated exact expressions for nonsymmetric rhabdoms, particularly over the range of parameters actually found in practice.

Fly-type (unfused) rhabdomeres

In the fly retina, the photoreceptors or rhabdomeres are separated, forming an unfused rhabdom (Fig. 2), cf.

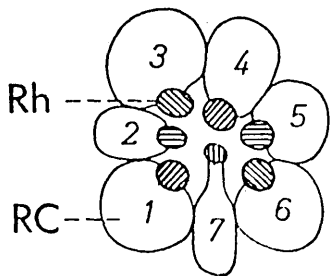


FIG. 2. Separated rhabdomeres (Rh) in a fly ommatidium. The dark lines represent the microvilli. RC are the retinula cells.

bee or ant. Fly rhabdomeres are known to be birefringent and dichroic,^{26,28} but as a result of the low PS values measured in rhabdomeres 1–6, it has been suggested that the dichroism of their microvillar medium is low (dichroic ratio $\Delta \sim 2$). An alternative scheme for low PS but which allows high dichroism of the microvillar medium, is for the rhabdomeres to twist.⁶ Although no direct evidence exists for *in situ* twisting of fly rhabdomeres, some twisting has been observed when sections are cut from the retina, probably as a result of disturbing the mechanical stability of the rhabdomeres (Boschek, personal communication). Therefore, even if twisting is not relevant to the visual process in the living animal, it may affect PS measurements on excised portions of the retina unless particular care is taken.²⁶ This will be examined in more detail in a later paper.

The propagation of light in a twisted fly-type rhabdomere is described directly by the theory of Sec. I (with the possible inclusion of waveguide effects which lower the effective absorption coefficient). Expressions for the absorption of light, the PS and direction of polarization for maximum absorption and the absorption of unpolarized light are given in Sec. A of the Appendix. We present in Fig. 3 results showing the effect of twisting on the PS and absorption of unpolarized light in a fly-type rhabdomere with various values of dichroic ratio and rhabdomere birefringence. In summary, we find that twisting of a fly rhabdomere tends to decrease its PS but to increase the absorption of unpolarized light.

Symmetric fused rhabdom

This case has been analyzed in Ref. 7. If the rhabdom as a whole is nondichroic and nonbirefringent, e.g., identical rhabdomeres with orthogonal microvilli as in Fig. 4, the direction of polarization of the electric field is unaffected by the twisting of the rhabdom. The absorption of both polarized and unpolarized light by the rhabdom as a whole, and the absorption of unpolarized light in the individual rhabdomeres are unaltered by the twisting. However the amount of linearly polarized light absorbed by a rhabdomere is changed because of the varying angle between the direction of polarization and the microvilli direction along the length of the twisting rhabdom. We find that the PS of a retinula cell is in general reduced by twisting of the rhabdom and that the angle for maximum absorption (i.e., the angle between the initial microvilli direction and the direction of po-

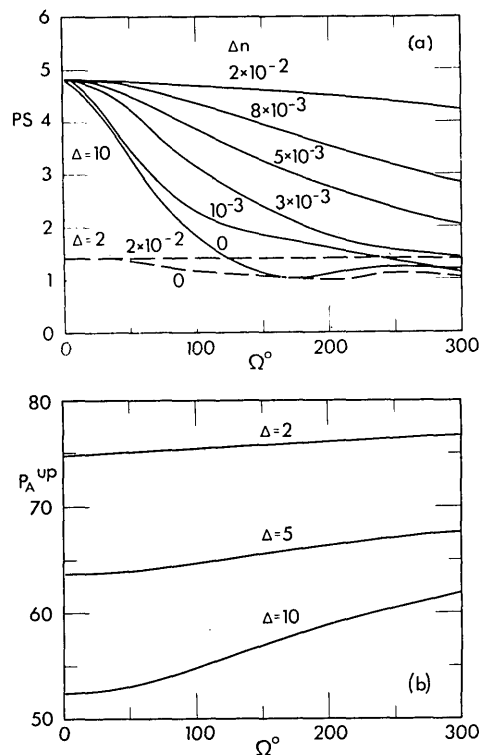


FIG. 3. The polarization sensitivity (a) and amount of unpolarized light absorbed in twisted fly-type rhabdomeres (b). $\alpha_0 l = 2$, $l = 200 \mu\text{m}$ and $\lambda = 500 \text{ nm}$ in (a) and (b), and $\Delta n = 3 \times 10^{-3}$ in (b).

larization) goes approximately as $\frac{1}{2}\Omega$ for small absorption, where Ω is the total twist angle of the rhabdom [for $0^\circ \leq \Omega < 180^\circ$; when $180^\circ < \Omega < 360^\circ$, the angle for maximum absorption $\approx \frac{1}{2}\Omega - 90^\circ$; Fig. 8(b) of Ref. 8 shows this incorrectly]. Exact formulas are given in Sec. B of the Appendix.

Anisotropic fused rhabdom with orthogonal microvilli

An example of this type of rhabdom is the worker bee²⁹ (Fig. 5). The optical axes of the rhabdom are along the two orthogonal microvilli axes but, because the rhabdomeres have different areas and absorption properties, the rhabdom birefringence and dichroism with respect to these axes are, in general, nonzero.³⁰ Expressions for this case are given in Sec. C of the Appendix. The rhabdom as a whole behaves like the fly rhabdomere, i.e., the absorption of unpolarized light is increased by the twisting, but the twisting again tends to destroy the PS of the individual retinula cells. The

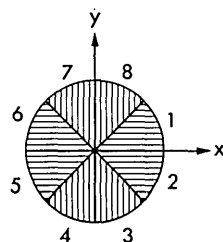


FIG. 4. A symmetric fused rhabdom. The rhabdomeres are assumed to be identical.

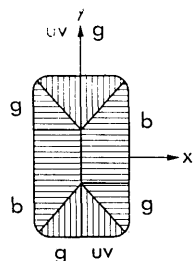


FIG. 5. An anisotropic fused rhabdom with orthogonal microvilli, as found in worker bee. uv (ultraviolet), b (blue), and g (green) indicate at which wavelengths the rhabdomeres absorb most strongly.

effect of twisting of the bee rhabdom is discussed in detail in Ref. 8.

Anisotropic fused rhabdom with nonorthogonal microvilli

In some cases, e.g., the rhabdoms of the bulldog ant³¹ and locust³² (Fig. 6), although the microvilli are not orthogonal, the symmetry of the rhabdom is such that the optical axes are orthogonal.³³ The absorption coefficients and the birefringence of the individual rhabdomeres must then be transformed from the coordinate axes parallel and perpendicular to the microvilli, to the optical axes using Eq. (A30), and summed as shown in Sec. D of the Appendix to give the overall birefringence and absorption coefficients of the rhabdom. These quantities are then used to calculate the electric field and the power absorbed in the rhabdomeres of the twisted rhabdom. The qualitative behavior of the PS and angle for maximum absorption is the same as for rhabdoms with orthogonal microvilli.

Symmetric-rhabdom approximation

The overall dichroism and birefringence of the fused rhabdom depends on the arrangement of the rhabdomeres within the rhabdom, as well as on the dichroism and birefringence of the rhabdomeric medium. Therefore, although the rhabdomeres may be dichroic ($\Delta n \approx 10$), and birefringent ($\Delta n \approx 4 \times 10^{-3}$), in many cases the symmetry of the rhabdom is such that the rhabdom as a whole is much less anisotropic. In these cases the symmetric-rhabdom expressions are often good approximations to the exact expressions. This is illustrated in Fig. 7, which compares the approximation with the exact values for several degrees of anisotropy. Provided that the rhabdom birefringence is less than about 4×10^{-4} , the approximate expression for the angle for maximum ab-

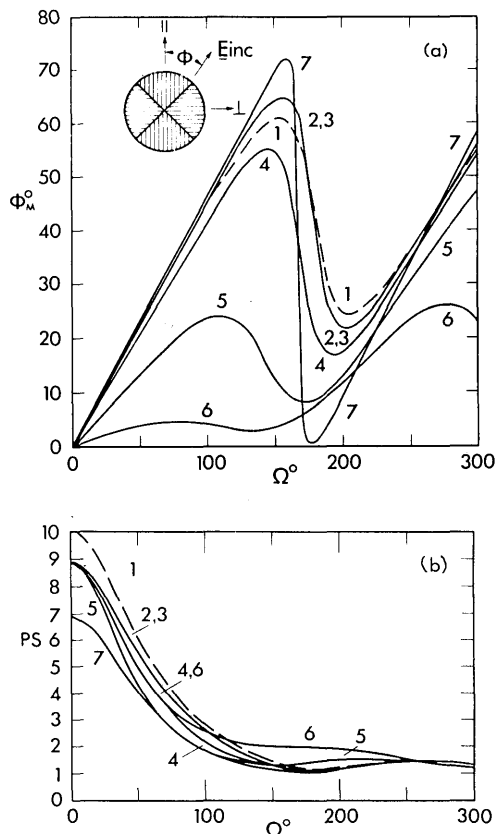


FIG. 7. Comparison of exact results (solid line) for an anisotropic rhabdom with orthogonal microvilli, with the symmetric-rhabdom approximation (curve 1—dashed line) for (a) the angle for maximum absorption ϕ_{max} , and (b) the polarization sensitivity, with the following rhabdom parameters:

Curve	Δn	γ_n/λ_L
1	0	1
2	0	1.67
3	1×10^{-4}	1.67
4	4×10^{-4}	1.67
5	8×10^{-4}	1.67
6	1.3×10^{-3}	1.67
7	4×10^{-4}	10

$\lambda = 350$ nm, the length of the rhabdom is $180 \mu\text{m}$, and $\frac{1}{2}(\gamma_n + \gamma_L)l = 0.5$. These parameters are approximately those of the worker-bee rhabdom.

sorption ϕ_{max} is accurate for most values of the twist angle Ω . The approximate expression for the PS is reasonably accurate even for relatively high values of the birefringence, but shows some error at small Ω for highly dichroic rhabdoms.

Layered rhabdoms

The fused rhabdom of the bee and of the ant consists of eight rhabdomeres which run for most of its length, and a ninth rhabdomere which lies underneath (and replaces) one or two of the eight in the lower or proximal third of the rhabdom.^{31,34} This layering is also found in the fly, in which rhabdomere 8 lies underneath rhabdomere 7.²⁸ The upper rhabdomere filters the light reaching the lower one, and this can lead to an enhancement of the PS of the underlying rhabdomere.²⁷ This has lent theo-

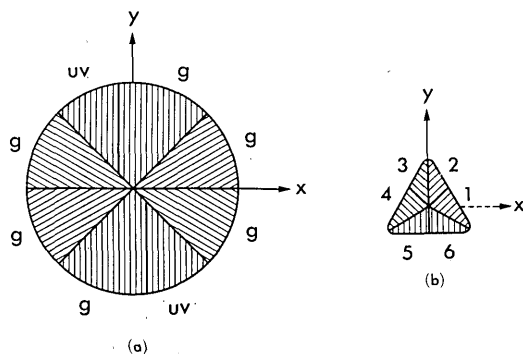


FIG. 6. Anisotropic fused rhabdoms with nonorthogonal microvilli (a) bulldog ant, (b) locust.

retical support to the hypothesis that the ninth cell in bee and in ant is specialized to polarization detection.³⁴

Twisting of the upper part of the rhabdom (or rhabdomere 7 in fly) will, however, tend to diminish this polarization-filter effect, which relies on the upper rhabdomere absorbing dichroically. This is discussed in Ref. 8 and will be examined in more detail than here in a later paper. To illustrate the effect we give an example using parameters typical of the ant rhabdom absorbing in the ultraviolet region of the spectrum,²³ and making use of the symmetric-rhabdom approximation, which we find to be valid when the total twist angle of the upper part of the rhabdom $\Omega \geq 20^\circ$. Table I shows the PS of the ninth cell, assuming that the lower portion of the rhabdom is short and does not twist significantly. Then, the PS of the ninth cell alone is approximately equal to the dichroic ratio Δ^{uv} of the uv-absorbing rhabdomeres.²⁷ Other parameters are $\gamma_{11}l = 0.5$ and $\Delta^{uv} = 10$. γ_{11} is the rhabdom absorption coefficient for light polarized parallel to the microvilli of the uv-absorbing rhabdomeres in the upper portion of the rhabdom, and l is the length of this portion. The value for $\Omega = 0^\circ$ is calculated using the theory of Ref. 34.

An outline of the procedure for calculating the power or number of photons absorbed in an underlying rhabdomere is given in Sec. E of the Appendix.

APPENDIX

The notation of the Appendix follows that of Refs. 6, 27, and 33.

A. Infinite medium—general expressions

Consider an infinite anisotropic medium, twisting at a rate of ξ about the z axis, with propagation constants β_x , β_y and absorption coefficients α_x , α_y along two orthogonal twisting coordinate axes in the plane orthogonal to the z axis (Fig. 1). The power (which is proportional to the number of photons) at any position z is given by

$$P(z) = \frac{1}{2} [|A_x(z)|^2 + |A_y(z)|^2] \quad (A1)$$

$$= \frac{1}{2} \{ \cosh 2S + \cosh 2S + |F| [1 + X^2 + Y^2 - 2Y \operatorname{Re}(pq^*)] (\cosh 2S - \cos 2R) - (pp^* - qq^*) [(Y \operatorname{Re} \sqrt{F} + X \operatorname{Im} \sqrt{F}) \sin 2R + (X \operatorname{Re} \sqrt{F} - Y \operatorname{Im} \sqrt{F}) \sinh 2S] \} e^{-\alpha_s z}, \quad (A2)$$

where

$$\begin{aligned} p &= A_x(0), \quad q = A_y(0), \quad X = (\beta_x - \beta_y)/2\xi, \\ Y &= (\alpha_x - \alpha_y)/4\xi, \quad R = \xi z \operatorname{Re}[1 + (X + iY)^2]^{1/2}, \\ S &= \xi z \operatorname{Im}[1 + (X + iY)^2]^{1/2}, \quad F = [1 + (X + iY)^2]^{-1} \end{aligned}$$

TABLE I. Polarization sensitivity of an underlying 9th cell. Parameters, typical of an ant rhabdom, are given in the text.

Ω°	PS ₉
0	15.7
20	11.2
40	10.3
60	10.1
80	10.1
100	10.1

and

$$\alpha_s = \frac{1}{2}(\alpha_x + \alpha_y).$$

The power absorbed between $z = 0$ and $z = l$ is given by

$$P_A(l) = P(0) - P(l). \quad (A3)$$

If the light is initially linearly polarized at an angle ϕ to $x(0)$, $p = \sqrt{2} \cos \phi$, $q = \sqrt{2} \sin \phi$ (assuming unit initial power). Then, maximizing Eq. (A3) with respect to ϕ gives the angle for maximum absorption ϕ_{\max} , i.e.,

$$\tan 2\phi_{\max} = M/N, \quad (A4)$$

where

$$M = |F| Y (\cosh 2S - \cos 2R), \quad (A5)$$

$$N = (Y \operatorname{Re} \sqrt{F} + X \operatorname{Im} \sqrt{F}) \sin 2R + (X \operatorname{Re} \sqrt{F} - Y \operatorname{Im} \sqrt{F}) \sinh 2S. \quad (A6)$$

The angle for minimum absorption ϕ_{\min} also satisfies Eq. (A4), so that the initial directions of polarization for maximum and minimum absorption are perpendicular in a linearly twisted medium.

Equations (A1)–(A6) may be used for twisted fly-type (unfused) rhabdomeres, with the waveguide parameter inserted as indicated in Sec. I if necessary (i.e., when $\eta < 1$). The polarization sensitivity PS is defined by

$$\text{PS} = [P_A(\phi = \phi_{\max})] / [P_A(\phi = \phi_{\min})]. \quad (A7)$$

The amount of unpolarized (UP) light absorbed is found by averaging over all ϕ , giving

$$P_A^{\text{UP}}(l) = \frac{1}{2} [\cos 2R + \cosh 2S + |F| (1 + X^2 + Y^2) (\cosh 2S - \cos 2R)] e^{-\alpha_s l} \quad (A8)$$

$$= \frac{1}{2} [P_A(\phi = \phi_{\max}) + P_A(\phi = \phi_{\min})]. \quad (A9)$$

Note that if we make the change $\Delta\alpha = \alpha_x - \alpha_y \rightarrow -\Delta\alpha$, then $\phi_{\max} \rightarrow \phi_{\min}$. Reversing the direction of the twist ($\xi \rightarrow -\xi$) changes the sign of ϕ_{\max} , whereas changing the sign of the birefringence ($\Delta\beta = \beta_x - \beta_y \rightarrow -\Delta\beta$) has no effect on ϕ_{\max} . In all cases PS remains unaltered.

At a given wavelength the number of photons is proportional to the power.

B. Symmetric-fused rhabdoms

If a fused rhabdom is nonbirefringent and nondichroic, light initially linearly polarized will remain linearly polarized in the initial direction as it propagates along the twisted rhabdom. The absorption by the rhabdom as a whole is therefore unaffected by the twist, but in general the absorption by the individual rhabdomeres is changed. This case has been analyzed in Refs. 6 and 7; we merely quote the results here because, as we show later, they are often a useful and simple approximation for twisted fused rhabdoms with less symmetry.

For light initially linearly polarized at an angle ϕ to the microvilli axis of rhabdomere j , the power absorbed by the rhabdomere is given by

$$P_A^j(\phi) = \left(\frac{\alpha_{||}^j + \alpha_{\perp}^j}{\gamma_s} \right) \left(\frac{A_j}{A} \right) \times \left\{ 1 - e^{-\gamma_s l} + \left(\frac{\alpha_{||}^j - \alpha_{\perp}^j}{\alpha_{||}^j + \alpha_{\perp}^j} \right) \left[1 + \left(\frac{2\xi}{\gamma_s} \right)^2 \right]^{-1} \right. \\ \times \left[e^{-\gamma_s l} \left(\frac{2\xi}{\gamma_s} \sin 2\theta - \cos 2\theta \right) + \frac{2\xi}{\gamma_s} \sin 2\phi + \cos 2\phi \right] \left. \right\}, \quad (\text{A10})$$

where $\alpha_{||}^j$, α_{\perp}^j are the absorption coefficients of rhabdomere j for light polarized parallel and perpendicular, respectively, to the microvilli axis, A_j is its cross-sectional area, A is the total rhabdom cross-sectional area, γ is the rhabdom absorption coefficient, given by

$$\gamma = \frac{1}{A} \sum_{\text{rhabdomeres}} A_j \alpha_j, \quad (\text{A11})$$

$\gamma_s = \frac{1}{2}(\gamma_{||} + \gamma_{\perp})$, where $\gamma_{||}$ (γ_{\perp}) is for light polarized parallel (perpendicular) to the microvilli of rhabdomere j , l is the length of the rhabdom and $\theta = \xi l - \phi$. We have assumed that the untwisted rhabdom does not change in size or structure along its length.

The angle for maximum (and minimum) absorption, found by differentiating Eq. (A10) with respect to ϕ , is given by

$$\tan 2\phi = \frac{2\xi/\gamma_s - e^{-\gamma_s l} [\sin 2\Omega + (2\xi/\gamma_s) \cos 2\Omega]}{1 + e^{-\gamma_s l} [(2\xi/\gamma_s) \sin 2\Omega - \cos 2\Omega]}, \quad (\text{A12})$$

where $\Omega = \xi l$. If $\gamma_s l \ll 1$ and $2\xi/\gamma_s \gg 1$, then $\phi_{\max} \approx \frac{1}{2}\Omega$ ($\Omega \leq \pi$).

The absorption of unpolarized light in both the rhabdom and the individual rhabdomeres is unaffected by twisting of the rhabdom.

$$(A/A_j)P_A^j(l) = \frac{1}{2}(\alpha_{||}^j + \alpha_{\perp}^j)[I_1 + (1 + X^2 + Y^2)I_2] - (\alpha_{||}^j - \alpha_{\perp}^j)[(Y \operatorname{Re}\sqrt{F} + X \operatorname{Im}\sqrt{F})I_3 - (Y \operatorname{Im}\sqrt{F} - X \operatorname{Re}\sqrt{F})I_4] \\ + \cos 2\phi \left\{ \frac{1}{2}(\alpha_{||}^j - \alpha_{\perp}^j)[I_1 - (1 - X^2 - Y^2)I_2] - (\alpha_{||}^j + \alpha_{\perp}^j)[(Y \operatorname{Re}\sqrt{F} + X \operatorname{Im}\sqrt{F})I_3 - (Y \operatorname{Im}\sqrt{F} - X \operatorname{Re}\sqrt{F})I_4] \right\} \\ + \sin 2\phi \{ (\alpha_{||}^j - \alpha_{\perp}^j)(I_3 \operatorname{Re}\sqrt{F} - I_4 \operatorname{Im}\sqrt{F}) - (\alpha_{||}^j + \alpha_{\perp}^j)YI_2 \}, \quad (\text{A17})$$

where here, $Y = (\gamma_x - \gamma_y)/4\xi$, and

$$I_1 = L + M, \quad (\text{A18})$$

$$I_2 = |F|(L - M), \quad (\text{A19})$$

$$L = \frac{e^{-\gamma_s l} (\gamma_s l \cosh 2S + 2S \sinh 2S) - \gamma_s l}{4S^2 - (\gamma_s l)^2}, \quad (\text{A20})$$

$$M = \frac{e^{-\gamma_s l} (-\gamma_s l \cos 2R + 2R \sin 2R) + \gamma_s l}{4R^2 + (\gamma_s l)^2}, \quad (\text{A21})$$

$$I_3 = \frac{2R - e^{-\gamma_s l} (\gamma_s l \sin 2R + 2R \cos 2R)}{4R^2 + (\gamma_s l)^2}, \quad (\text{A22})$$

$$I_4 = \frac{e^{-\gamma_s l} (\gamma_s l \sinh 2S + 2S \cosh 2S) - 2S}{4S^2 - (\gamma_s l)^2}. \quad (\text{A23})$$

Equations (A17)–(A23) reduce to Eq. (A10) when $X = Y = 0$. Equation (A17) is of the form $P_A^j(l) = A + B \cos 2\phi + C \sin 2\phi$, so that the angles for maximum and minimum absorption are solutions of

$$\tan 2\phi = C/B, \quad (\text{A24})$$

C. Anisotropic fused rhabdom with orthogonal microvilli

Following Ref. 33, we now generalize to the case in which the untwisted rhabdom has orthogonal microvilli but is birefringent and dichroic with respect to the optical axes, which are aligned along the microvilli axes. The power at any position z along the twisted rhabdom is given by Eq. (A1), with the propagation constants and absorption coefficients those of the rhabdom. To find the power absorbed in a rhabdomere we use^{33,35}

$$P_A^j(l) = \frac{\omega}{2} \operatorname{Im} \int_{V_j} \mathbf{E} \cdot \boldsymbol{\epsilon} \cdot \mathbf{E}^* dV, \quad (\text{A13})$$

where V_j is the volume of the medium, i.e., rhabdomere j , ω is the circular frequency, and $\boldsymbol{\epsilon}$ is the dielectric tensor of the medium, which in this case is of the form

$$\boldsymbol{\epsilon} = \begin{pmatrix} \epsilon_x & 0 \\ 0 & \epsilon_y \end{pmatrix}.$$

In the previous section $\epsilon_x = \epsilon_y$. Substitution into Eq. (A13) gives

$$P_A^j(l) = (A_j/A)(\alpha_{||}^j I_{||} + \alpha_{\perp}^j I_{\perp}). \quad (\text{A14})$$

where

$$I_{||} = \int_0^l |A_x(z)|^2 dz, \quad (\text{A15})$$

$$I_{\perp} = \int_0^l |A_y(z)|^2 dz. \quad (\text{A16})$$

We have taken the x axis parallel to the microvilli of rhabdomere j . Evaluation of the integrals using Eqs. (9) and (10) leads to

and the absorption of unpolarized light is given by

$$P_A^j(l)_{\text{UP}} = A. \quad (\text{A25})$$

Equations (A17)–(A25) simplify if either the birefringence or dichroism is zero.

D. Anisotropic fused rhabdom with nonorthogonal microvilli

Again following Ref. 33, we proceed to the case in which the microvilli are nonorthogonal but the optical axes of the untwisted rhabdom remain perpendicular. In this case the dielectric tensor is of the form

$$\boldsymbol{\epsilon} = \begin{pmatrix} \epsilon_x & \epsilon_{xy} \\ \epsilon_{xy} & \epsilon_y \end{pmatrix}, \quad (\text{A26})$$

and the power absorbed in an individual rhabdomere of the form

$$P_A^j = P_s^j + P_c^j, \quad (\text{A27})$$

where $P_s^j(l)$ is given by Eqs. (A17)–(A23) but with all parameters now referred to the x and y (optical) axes, rather than to the \parallel and \perp axes, and

$$P_c^j(l) = \frac{1}{2} \frac{A_l}{A} \alpha_{xy}^j \operatorname{Re} \int_0^l A_x^*(z) A_y(z) dz \quad (\text{A28})$$

$$= \frac{\alpha_{xy}^j}{2} \frac{A_l}{A} \{ Y I_2 - \cos 2\phi (I_3 \operatorname{Re} \sqrt{F} + I_4 \operatorname{Im} \sqrt{F}) + \frac{1}{2} \sin 2\phi [I_1 - (1 + X^2 + Y^2) I_2] \}. \quad (\text{A29})$$

$I_1 - I_4$ are given by Eqs. (A18)–(A23).

The rhabdomere absorption coefficients α_x^j , α_y^j , α_{xy}^j are found from α_{\parallel}^j , α_{\perp}^j by a change of basis as described in Appendix D of Ref. 33. There it is shown that

$$\begin{pmatrix} \alpha_{\parallel}^j & 0 \\ 0 & \alpha_{\perp}^j \end{pmatrix}_{\parallel, \perp}$$

transforms to

$$\begin{pmatrix} \alpha_x^j & \alpha_{xy}^j \\ \alpha_{xy}^j & \alpha_y^j \end{pmatrix}_{x, y} = \begin{pmatrix} \alpha_{\parallel}^j \cos^2 \theta_j + \alpha_{\perp}^j \sin^2 \theta_j & -(\alpha_{\parallel}^j - \alpha_{\perp}^j) \sin \theta_j \cos \theta_j \\ -(\alpha_{\parallel}^j - \alpha_{\perp}^j) \sin \theta_j \cos \theta_j & \alpha_{\parallel}^j \sin^2 \theta_j + \alpha_{\perp}^j \cos^2 \theta_j \end{pmatrix}_{x, y}, \quad (\text{A30})$$

where θ_j is the angle between the x axis and the microvilli axis of rhabdomere j . The rhabdom absorption coefficients γ_x , γ_y are then found from Eq. (A11), using the appropriate, transformed, rhabdomere absorption coefficients.

The birefringence of the rhabdom can also be found from the birefringence of the individual rhabdomeres. Provided that the birefringence $\Delta n_j \ll n_j$ (the average refractive index of the rhabdomere), Δn_j transforms like α^j , i.e., according to Eq. (A30). From the theory of Ref. 33, it can be shown that the birefringence of the rhabdom, for the purposes of this theory, is given by a weighted integral over the individual birefringences, which for a uniform field, reduces to a sum like Eq. (A11), i.e.,

$$\Delta n = \frac{\eta}{A} \sum_{\text{rhabdomeres}} A_j \Delta n_j, \quad (\text{A31})$$

where the birefringence of the rhabdom $\Delta n = n_x - n_y$ and the Δn_j are all with respect to the $x - y$ axes.

In the limit of no twist ($\xi \rightarrow 0$), the expressions Eqs. (A21)–(A29) reduce to those given in Refs. 33 and 30.

The extension of the theory to the case of nonorthogonal optical axes is straightforward but more lengthy. The reader is referred to Ref. 33 for details.

E. Layered rhabdoms

The absorption in the first layer is calculated as shown in Secs. A–D of this Appendix. The values of $A_x(l_1)$, $A_y(l_1)$, where l_1 is the length of the first layer, are evaluated from Eqs. (9)–(15) and then used as the initial values p , q for the next layer. The absorption in this layer is again calculated using the appropriate expressions in Secs. A–D of this Appendix, but with $\sin 2\phi$

replaced by $\operatorname{Re}(pq^*)$ and $\cos 2\phi$ by $\frac{1}{2}(pp^* - qq^*)$. The expressions for the angle for maximum absorption and PS of the second layer will generally be more complicated than those for just one layer because of the larger number of parameters involved, and in this case the symmetric-rhabdom approximation may prove especially useful.

The calculations can be repeated for any number of layers.

ACKNOWLEDGMENT

One of us (P.M.) is grateful to C.S.I.R.O. for financial support and to Professor K. Kirschfeld for helpful comments and the invitation to work at the Max-Planck-Institut für biologische Kybernetik. We also thank Manfred Heusel for preparing the diagrams.

- ¹A. R. Stokes, *The Theory of the Optical Properties of Inhomogeneous Materials* (Spon Press, London, 1963).
- ²H. L. deVries, "Rotatory power and other optical properties of certain liquid crystals," *Acta Crystallogr.* **4**, 219 (1951).
- ³A. S. Marathay, "Matrix-operator description of the propagation of polarized light through cholesteric liquid crystals," *J. Opt. Soc. Am.* **61**, 1363 (1971).
- ⁴D. W. Berreman, "Optics in stratified and anisotropic media: 4×4 matrix formulation," *J. Opt. Soc. Am.* **62**, 502 (1972); D. W. Berreman, "Optics in smoothly varying planar structures: Applications to liquid-crystal twist cells," *J. Opt. Soc. Am.* **63**, 1374 (1973).
- ⁵R. M. A. Azzam and N. M. Bashara, "Simplified approach to the propagation of polarized light in anisotropic media—application to liquid crystals," *J. Opt. Soc. Am.* **62**, 1252 (1972).
- ⁶P. D. McIntyre, "Crosstalk between optical waveguides with applications to visual photoreceptors," Ph. D. thesis (Australian National University, Canberra, Australia, 1976).
- ⁷A. W. Snyder and P. D. McIntyre, "Polarization sensitivity of twisted fused rhabdoms," in *Photoreceptor Optics*, edited by A. W. Snyder and R. Menzel (Springer-Verlag, Heidelberg, 1975).
- ⁸R. Wehner, G. D. Bernard, and E. Geiger, "Twisted and non-twisted rhabdoms and their significance for polarization detection in the bee," *J. Comp. Physiol.* **104**, 225 (1975).
- ⁹C. Mauguin, *Bull. Soc. Fr. Mineral.* **34**, 71 (1911), quoted in Ref. 2.
- ¹⁰C. Hu and J. R. Whinery, "Losses of a nematic liquid-crystal optical waveguide," *J. Opt. Soc. Am.* **64**, 1424 (1974).
- ¹¹W. H. Louisell, *Coupled Modes and Parametric Electronics* (Wiley, New York, 1960).
- ¹²A. W. Snyder, "Coupling of modes on a tapered dielectric cylinder," *IEEE Trans. Microwave Theory Tech.* **MTT-18**, 383 (1970).
- ¹³A. Reisinger, "Characteristics of optical guided modes in lossy waveguides," *Appl. Opt.* **12**, 1015 (1973).
- ¹⁴A. W. Snyder, "Asymptotic expressions for eigenfunctions and eigenvalues of a dielectric or optical waveguide," *IEEE Trans. Microwave Theory Tech.* **MTT-17**, 1130 (1969).
- ¹⁵P. D. McIntyre and A. W. Snyder, "Power transfer between optical fibers," *J. Opt. Soc. Am.* **63**, 1518 (1973).
- ¹⁶A. W. Snyder, "Power loss on optical fibers," *Proc. IEEE* **60**, 757 (1972).
- ¹⁷A. W. Snyder, "Leaky-ray theory of optical waveguides of circular cross-section," *Appl. Phys.* **4**, 273 (1974).
- ¹⁸The ellipticity is defined as the ratio of the lengths of the major and minor axes of the polarization ellipse. The usual symbol is η but here we use σ to avoid confusion with the waveguide parameter η .
- ¹⁹M. Born and E. Wolf, *Principles of Optics*, 2nd ed. (Perga-

- mon, New York, 1970).
- ²⁰D. Clarke and J. F. Grainger, *Polarized Light and Optical Measurement* (Pergamon, Oxford, 1971).
- ²¹O. J. Grundler, "Elektronenmikroskopische Untersuchungen am Auge der Honigbiene (*Apis mellifera*)," *Cytobiol.* **9**, 203 (1974).
- ²²R. Menzel, "Polarisation Sensitivity in Insect Eyes with Fused Rhabdoms," in *Photoreceptor Optics*, edited by A. W. Snyder and R. Menzel (Springer-Verlag, Heidelberg, 1975).
- ²³R. Menzel and M. Blakers, "Functional organisation of an insect ommatidium with fused rhabdom," *Cytobiol.* **11**, 279 (1975).
- ²⁴J. N. Israelachvili, R. A. Sammut, and A. W. Snyder, "Birefringence and dichroism of photoreceptors," *Vis. Res.* **16**, 47 (1976).
- ²⁵A. W. Snyder and S. B. Laughlin, "Dichroism and absorption by photoreceptors," *J. Comp. Physiol.* **100**, 101 (1975).
- ²⁶K. Kirschfeld and A. W. Snyder, "Waveguide Mode Effects, Birefringence and Dichroism in Fly Photoreceptors," in *Photoreceptor Optics*, edited by A. W. Snyder and R. Menzel (Springer-Verlag, Heidelberg, 1975).
- ²⁷A. W. Snyder, "Polarization sensitivity of individual retinula cells," *J. Comp. Physiol.* **83**, 331 (1973).
- ²⁸K. Kirschfeld, "The Visual System of *Musca*: Studies on Optics, Structure and Function," in *Information Processing in the Visual System of Arthropods*, edited by R. Wehner (Springer-Verlag, Berlin, 1972).
- ²⁹F. G. Gribakin, "Cellular basis of colour vision in the honey bee," *Nature* **223**, 639 (1969).
- ³⁰A. W. Snyder and R. A. Sammut, "Direction of *E* for maximum response of a retinula cell," *J. Comp. Physiol.* **85**, 37 (1973).
- ³¹R. Menzel, "The Fine Structure of the Compound Eye of *Formica polyctena*-Functional Morphology of a Hymenopteran Eye," in *Information Processing in the Visual System of Arthropods*, edited by R. Wehner (Springer-Verlag, Berlin, 1972).
- ³²G. A. Horridge, "The Retina of the Locust," in *The Functional Organization of the Compound Eye*, edited by C. G. Bernhard (Pergamon, Oxford, 1966).
- ³³A. W. Snyder, "Light absorption in visual photoreceptors," *J. Opt. Soc. Am.* **64**, 216 (1974).
- ³⁴R. Menzel and A. W. Snyder, "Polarized light detection in the bee, *Apis mellifera*," *J. Comp. Physiol.* **88**, 247 (1974).
- ³⁵R. P. Feynman, R. B. Leighton, and M. Sands, *Lectures on Physics* (Addison-Wesley, Reading, Mass., 1963), Vol. 1, p. 33. S. G. Lipson and H. Lipson, *Optical Physics* (Cambridge U. P., Cambridge, England, 1962). L. D. Landau and E. M. Lifshitz, *Electrodynamics of Continuous Media* (Pergamon, Oxford, 1963).

Image mensuration by maximum *a posteriori* probability estimation*

James W. Burnett[†] and Thomas S. Huang

School of Electrical Engineering, Purdue University, West Lafayette, Indiana 47907

(Received 26 August 1977)

We present an algorithm for pulse width estimation from blurred and nonlinear observations in the presence of signal dependent noise. The main application is the accurate measurement of image sizes on film. The problem is approached by modeling the signal as a discrete position finite state Markov process, and then determining the transition location that maximizes the *a posteriori* probability. It turns out that the blurred signal can be represented by a trellis, and the maximum *a posteriori* probability (MAP) estimation is obtained by finding the minimum cost path through the trellis. The latter is done by the Viterbi algorithm. Several examples are presented. These include the measurement of the width of a road in an aerial photo taken at an altitude of 5000 ft. The resulting width estimate is accurate to within a few inches.

I. INTRODUCTION

This work presents an algorithm for pulse width estimation from blurred and nonlinear observations in the presence of signal-dependent noise. The problem is motivated by the need for accurate measurements from remotely sensed photographs.

The problem is approached by modeling the signal (reflected light intensity) as a discrete position finite state Markov process. Sample functions of such a process are graphically represented by a path through a trellis. Blurred versions of these signals are similarly represented. By assigning a cost or length to each branch of the trellis a MAP sequence estimate of the signal is computed by finding the minimum cost or minimum length path through the trellis. MAP sequence estimates produced in this fashion have unambiguous edge locations making them useful for pulse width measurements.

The Viterbi algorithm is introduced as an efficient means of finding the minimum cost path through the trellis. The performance of the algorithm at locating step edges and measuring pulse widths is analyzed. When the possible states are known *a priori* the algorithm is shown to produce asymptotically unbiased, minimum variance discrete width estimates. The decrease in performance is slight if the true states are unknown and estimates (obtained from the available data) used in their place.

Computer simulation results show the variance of the discrete estimates is close to the Cramer-Rao bound. The algorithm is applied to the measurement of a road in an aerial photo taken at an altitude of 5000 ft. The resulting width estimate is accurate to within a few inches. Experimental results also indicate the estimates are not sensitive to small variations in the degrading system. Finally, it is shown how the discrete position model can be used to measure the radius of a cylinder in the presence of a nuisance parameter.